

# Theoretical Aspects on bound states, virtual states and resonances from the Friedrichs model

---

Zhiguang Xiao<sup>a,\*</sup> and Zhi-Yong Zhou<sup>b</sup>

<sup>a</sup>*School of Physics, Si Chuan University, Chengdu 610065, P. R. China*

<sup>b</sup>*School of Physics, Southeast University, Nanjing 211189, P. R. China*

*E-mail:* [xiaozg@scu.edu.cn](mailto:xiaozg@scu.edu.cn)

Friedrichs-Lee model is a model which couples the bare discrete states with the bare continuum states, where the exact solutions of the bound states, resonances and virtual states can be solved. We review how to use the exact solutions to understand some theoretical aspects of the resonances, virtual states and bound states. In particular, we show that the integration contours in the solutions make the norms for the resonances and virtual states not well-defined, new discrete states can be dynamically generated from the singularity of the form factors, and the behaviors for the near threshold states for the S-waves and higher partial waves can be different. We also review some applications of this model in discussing the properties the hadron spectrum.

*The 10th International workshop on Chiral Dynamics*  
*15-19 November 2021*  
*Beijing, China*

---

\*Speaker

## 1. Introduction

To understand the hadron spectrum is a main task in understanding the strong interaction. The quark potential models which partially incorporate the effective interaction from QCD have achieved a general success in predicting many meson states with different quantum numbers [1, 2]. However, above the open flavor threshold, there are severe deviations of the predictions from the experiments. In recent years, a lot of XYZ states were discovered in the experiments which may not have the conventional  $q\bar{q}$  state explanation. To understand the origins of these states is an important problem to be addressed.

The naïve classification of the hadronic states is to use their quark components like  $q\bar{q}$  for meson states,  $qqq$  for Baryon states, and tetraquarks, etc. In the scattering of these states, there could be bound states, virtual states or resonances as the intermediate states. In fact, lots of states in the experiments are discovered as resonances. In general, when a state appears as the intermediate state of the scattering of two hadronic states, it may not be pure fundamental one like  $q\bar{q}$  state, but may also contain higher Fock space components such as two-hadron continuum components. Besides, some states are proposed to be pure composite ones which have only the continuum components. How to describe these states in terms of these components is a theoretical interesting problem.

To understand these states is hard in the real world situation, however, by analysing a solvable model one can grasp some main properties of the intermediate states and gain further insights to the states in the real world. We will look at a solvable model — the Friedrichs-Lee model. The original idea of the Friedrichs model is that, when a discrete state is coupled to an opened continuum channel, the discrete state will dissolve into the continuum and becomes a resonant state [3]. Then the discrete state solutions for the full Hamiltonian can be exactly solved. There are also other models implementing similar idea in various areas in physics, such as in atomic physics [4] and in quantum optics [5]. The Lee model is an implementation in the QFT to study the renormalization [6]. The Friedrichs-Lee model is also linked to quantum field theory (QFT) model in [7] and thermal systems [8]. From the exact solution of this model, we will try to make some observations of the properties of the intermediate bound states, virtual states and resonances, which are helpful in understanding the hadron spectrum. This model can also be applied to the real world hadron spectrum analysis and produce some interesting results.

## 2. Bound state, virtual state and resonances in Friedrichs model

In this section, we review some basic facts of the Friedrichs model [3] and some of its generalizations developed in [9–11]. The simplest version of the Friedrichs model consist in a discrete state  $|0\rangle$ , a continuum  $|\omega\rangle$ , and the interaction between them. The full

Hamiltonian  $H$  is separated into a free part  $H_0$  and an interaction part  $V$  as

$$H = H_0 + V, \quad H_0 = \omega_0 |0\rangle\langle 0| + \int_{\omega_{th}}^{\infty} \omega |\omega\rangle\langle \omega| d\omega, \quad (1)$$

$$V = \lambda \int_{\omega_{th}}^{\infty} [f(\omega) |\omega\rangle\langle 0| + f^*(\omega) |0\rangle\langle \omega|] d\omega, \quad (2)$$

$$\text{with } \langle 0|0\rangle = 1, \langle \omega|\omega'\rangle = \delta(\omega - \omega'), \langle 0|\omega\rangle = \langle \omega|0\rangle = 0, \quad (3)$$

where the  $\omega_0$  denotes the energy for the free discrete state, and  $\omega \in [\omega_{th}, \infty)$  the energy range for the free continuum state,  $\omega_{th}$  being the threshold for the continuum states.  $f(\omega)$  function is the coupling vertex between the discrete state and the continuum state, and  $\lambda$  denotes the coupling strength. The eigenvalue problem for the full Hamiltonian can be exactly solved and the solutions include a continuum spectrum and a discrete spectrum. The final generalized eigenstates of the continuum spectrum with eigenvalue  $E > \omega_{th}$  can be expressed as

$$|\Psi_{\pm}(E)\rangle = |E\rangle + \lambda \frac{f(E)}{\eta^{\pm}(E)} \left[ |0\rangle + \lambda \int_{\omega_{th}}^{\infty} d\omega \frac{f(\omega)}{E - \omega \pm i\epsilon} |\omega\rangle \right], \quad (4)$$

$$\text{where } \eta^{\pm}(x) = x - \omega_0 - \lambda^2 \int_{\omega_{th}}^{\infty} \frac{f(\omega)f^*(\omega)}{x - \omega \pm i\epsilon} d\omega, \quad \langle \Psi_{\pm}(E)|\Psi_{\pm}(E')\rangle = \delta(E - E'). \quad (5)$$

The subscript  $\pm$  denotes the in-states (+) and outstates (-), respectively. The  $S$ -matrix can then be obtained as

$$S(E, E') = \delta(E - E') \left( 1 - 2\pi i \frac{\lambda f(E)f^*(E)}{\eta^+(E)} \right). \quad (6)$$

The  $\eta^{\pm}$  function can be analytically continued to the complex plane to be one complex function  $\eta(z)$  for  $z \in \mathbb{C}$  with a cut on  $E > \omega_{th}$ , with  $\eta(x \pm i\epsilon) = \eta^{\pm}(x)$  for  $x > \omega_{th}$  at the upper or the lower edge of the cut. Continued through the cut,  $\eta(z)$  can be defined on a two-sheeted Riemann surface. From Eq. (6), the zero points for the  $\eta(z) = 0$  will be the poles for the  $S$ -matrix. As expected, by directly solving the eigenvalue problem, the generalized discrete eigenvalues for the full Hamiltonian are just the zero points of  $\eta(z)$ . Usually, for hermitian Hamiltonian, there are only real eigenvalues for the normalizable eigenvectors in the Hilbert space. However, the zero points of  $\eta$  obviously can have complex solutions, which correspond to the non-normalizable state vectors and are called the generalized eigenstates for the Hamiltonian. Depending on the position of the solution on the double-sheeted Riemann surface, different kinds of the discrete generalized eigenstates can be found:

### 1. Bound state.

The solution to  $\eta(z) = 0$  on the real axis of the first sheet with  $z < \omega_{th}$  represents a bound state. The solution for a bound state at  $z_B$  is expressed as

$$|z_B\rangle = N_B \left( |0\rangle + \lambda \int_{\omega_{th}}^{\infty} \frac{f(\omega)}{z_B - \omega} |\omega\rangle d\omega \right). \quad (7)$$

This state has a finite norm and can be normalized as  $\langle z_B | z_B \rangle = 1$  when

$$N_B = (\eta'(z_B))^{-1/2} = \left( 1 + \lambda^2 \int d\omega \frac{|f(\omega)|^2}{(z_B - \omega)^2} \right)^{-1/2}.$$

Thus, as expected, this is a well-defined eigenstate of the Hamiltonian in the Hilbert space. Then, it is easy to define the so-called ‘‘elementariness’’  $Z$  which means the probability of finding the original bare discrete state in the bound state, and also the ‘‘compositeness’’  $X$ , the probability for finding the original continuum states in the bound state, the same as what Weinberg did[12]

$$Z = N_B^2, \quad X = \lambda^2 N_B^2 \int d\omega \frac{|f(\omega)|^2}{(z_B - \omega)^2}. \quad (8)$$

## 2. Virtual state.

If the solution lies on the real axis below the threshold on the second sheet, it represents a virtual state. The state for the solution can be expressed as

$$|z_V^\pm\rangle = N_V \left( |0\rangle + \lambda \int_{\omega_{th}}^{\infty} \frac{f(\omega)}{[z_V - \omega]_\pm} |\omega\rangle d\omega \right), \quad (9)$$

where the  $[\dots]_\pm$  means the analytical continuations of the integration from upper edge (+) and lower edge (–) of the cut to the second sheet [9]. The analytic continuation can be done by deforming the integration contour from the upper side (+) or the lower side (–) of cut on the first sheet to the second sheet, enclosing the virtual state pole position. See Fig. 1 for an illustration of the contour for  $|z_V^+\rangle$ . Since the physical region is on the upper edge of the cut, we take  $|z_V^+\rangle$  as a standard representation for the virtual state which is continued from the upper edge. Unlike the bound state, virtual state does not have a well-defined norm as the usual states in the Hilbert space, due to the different integration contours for  $\langle z_V^+|$  and  $|z_V^+\rangle$  from Eq. (9). Thus, it is not a well-defined state in Hilbert space. As a result, the compositeness and elementariness for the virtual state can not be mathematically rigorously defined as usual. However, since the integral contours for  $\langle z_V^-|$  and  $|z_V^+\rangle$  are the same, we can define a normalization such that  $\langle z_V^- | z_V^+ \rangle = 1$ , by choosing  $N_V = \langle z_V^- | z_V^+ \rangle = (\eta'^+(z_V))^{-1/2} = \left( 1 + \lambda^2 \int d\omega \frac{|f(\omega)|^2}{[z_V - \omega]_+^2} \right)^{-1/2}$ . However, it is not guaranteed that  $N_V$  is positive definite, because of the detoured integration path.

## 3. Resonant state.

If there is a solution in complex plane of the second Riemann sheet there must be another pole at the mirror image with respect to the real axis because of the real analyticity of  $\eta$  function. This pair of poles represent a resonance since it is unstable due to the finite imaginary part of the energy eigenvalue. The pole position close to

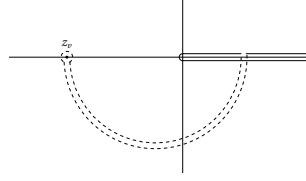


**Figure 1:** The example integration contour for the virtual state and resonant state.

the physical region is related to the mass  $M$  and width  $\Gamma$  as  $z = M - i\frac{\Gamma}{2}$ . The states for the two poles can be expressed as

$$|z_R\rangle = N_R \left( |0\rangle + \lambda \int_{\omega_{th}}^{\infty} d\omega \frac{f(\omega)}{[z_R - \omega]_+} |\omega\rangle \right), \quad |z_R^*\rangle = N_R^* \left( |0\rangle + \lambda \int_{\omega_{th}}^{\infty} d\omega \frac{f^*(\omega)}{[z_R^* - \omega]_-} |\omega\rangle \right), \quad (10)$$

where  $z_R$  is on the lower half plane and  $z_R^*$  is its complex conjugate. Similar to the virtual states, the resonance states can not be normalized as usual, and thus are not the normal state vector in the Hilbert space. However we can also choose

$$N_R = (\eta^{t+}(z_R))^{-1/2} = \left( 1 + \lambda^2 \int_{\omega_{th}}^{\infty} d\omega \frac{|f(\omega)|^2}{[(z_R - \omega)_+]^2} \right)^{-1/2} \quad (11)$$

to normalize the state as  $\langle z_R^* | z_R \rangle = 1$ . Notice that the normalization  $N_R$  will be complex in general. By summing up the perturbation series, I. Prigogine and his collaborators also obtained similar solutions [13].

### 3. Properties of bound states, virtual states and resonances

The bound states can be generated in two ways. The first is when  $\omega_0 < \omega_{th}$  with a small enough coupling, the position of the original discrete state is renormalized and the bound state pole is just shifted a little from  $\omega_0$  on the real axis of the first sheet. The second way is that for a large attractive coupling, there could be virtual state pole coming up from the second sheet to the first sheet and becoming a bound state pole, or there could be resonance poles that meet at the threshold and become a bound state and a virtual state. We will see examples later.

If  $\omega_0 > \omega_{th}$ , when the coupling is turned on the discrete state pole will move onto the complex plane of the second Riemann sheet and become a pair of resonance poles. Another way for a resonant state to appear is that it can be dynamically generated as an intrinsic nonperturbative phenomenon. In general, the dynamically generated pole is the result of the interaction form factor, i.e. it is related to the singularities of the form factor. Usually, this kind of pole comes from faraway and moves near to the physical region at a strong coupling.

The virtual states could be generated also in different ways. The first way is that it appears as the accompanying shadow pole of the bound state generated from the original

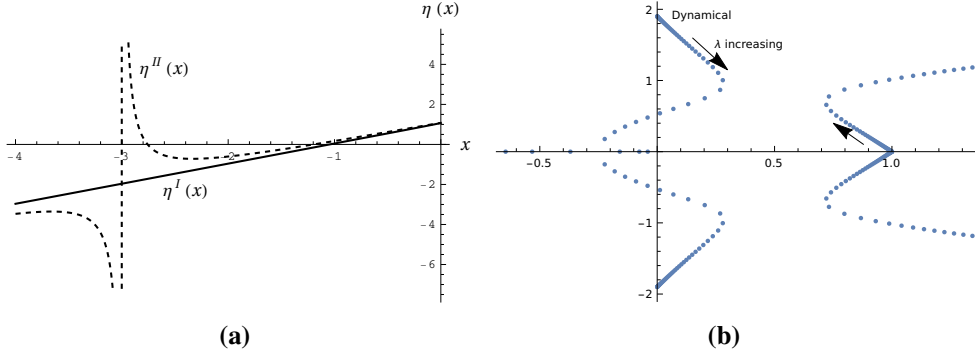


**Figure 2:** (a) An example  $\eta$  function on the first sheet and second sheet when  $\omega < \omega_{th}$  and the coupling is small. Here,  $\omega_{th} = 0$ ,  $\omega_0 = -1$ . There is also a simple pole of the form factor  $G(\omega)$  at  $\omega = -3$ . (b) An example pole trajectory for the dynamically generated resonance poles from the singularity of the form factor. The poles for the form factor are at  $\pm i1.9$ . The pole for the bare state is at 1.0.

discrete state when the coupling is small enough and  $\omega_0 < \omega_{th}$ . This can be easily seen from the analytically continued  $\eta(z)$  function,

$$\eta^I = z - \omega_0 - \lambda^2 \int_0^\infty \frac{|f(\omega)|^2}{z - \omega} d\omega \quad (12)$$

$$\eta^{II}(\omega) = \eta^I(\omega) + 2\pi i \lambda^2 G^{II}(\omega) = \eta^I(\omega) - 2\lambda^2 \pi i G(\omega), \quad (13)$$

where  $G(\omega) = |f(\omega)|^2$  and the superscript  $I$  and  $II$  denotes the first and the second sheet. Since in general  $G(\omega)$  is proportional to the imaginary part of  $\eta$  function for  $\omega > \omega_{th}$ , in most physical applications, it would be an anti-analytic function, i.e.  $G^*(\omega) = -G(\omega^*)$ , and  $2\pi i G(\omega)$  would be real below the threshold. When  $\lambda$  is small, on the first sheet, the integral term, which is real and negative, only deforms the  $\eta$  function a little, thus shift the bound state pole position from  $\omega_0$  a little. On the second sheet, since  $2\lambda^2 \pi i G(\omega)$  is real in (13), near  $\omega_0$  the  $\eta$  function is also shifted a little, and there should be a zero point to  $\eta^{II}$  near  $\omega_0$ , which means that the bound state would always accompanied with a virtual shadow pole. See Fig. 2(a) for an illustration.

The virtual states could also be generated from the form factor. This is also illustrated in Fig. 2(a) where there is a simple pole of the form factor at  $\omega = -3$ . We can see that there is a pole for the  $\eta^{II}$  at the position of the form factor  $G(\omega)$  from Eq. (13). This further produce a zero point for  $\eta^{II}$  and hence generates the dynamical virtual state. There could also be dynamically generated resonances from the poles of form factor (Fig2(b)). For the exponential form factor, similar dynamical poles could be generated from infinity. See [9, 10] for detailed discussions.

Thus we see that, in general, there could be states dynamically generated from the singular points of the form factor. Since this kind of dispersion relation also appears in other widely used models, the above discussion also applies to these models.

All the discrete states, whether dynamically generated or originated from the bare ones are represented as in Eq. (7), (9), (10). Since in these equations the continuum components are multiplied by  $\lambda$ , one may wonder whether in the  $\lambda \rightarrow 0$  limit, all the discrete state solutions tend to the bare ones. For the states generated from the bare states, it is true. But for the dynamical ones, this is not the case. The point is that the pole positions for the dynamically generated poles also depends on  $\lambda$  and as  $\lambda \rightarrow 0$  they tends to the singular points of the  $G(\omega)$ . This causes the integral to be divergent and the singularity cancels the coefficient  $\lambda$ . Thus at  $\lambda \rightarrow 0$  limit, the continuum part would not vanish, and the states does not tend to the bare discrete states because of the singularities in the integral.

Consequently, there is a caveat for a common practice of using the form factor put by hand when unitarizing the Chiral perturbation or other perturbative results. Usually, people start from a perturbation calculation from a Lagrangian model and use an exponential or monopole form factor put by hand to impose a high energy suppression of the perturbative result. Then after the unitarization they found a dynamically generated state and claim that there is a state dynamically generated by their Lagrangian model. From the above discussion, we see that the form factor alone can dynamically generate states. There could be a possibility that the dynamical state they found is generated not from their Lagrangian model by itself but from the form factor which is put by hand and has no dynamical origin from the Lagrangian. Thus the claim that the Lagrangian model generates the dynamical state would be suspicious.

It is important to emphasize that in the expressions for virtual states and resonant states, the integral contour should be deformed since the pole positions are located on the second sheet. This is the reason why the state can not be normalized as usual, since the multiplication for two distributions may not be well-defined. For the resonance, in fact, the usually defined norm  $\langle z_R | z_R \rangle$  can be evaluated by a manipulation of the integration and turns out to be exactly zero. A simple argument is that for  $\langle z_R | H | z_R \rangle$ ,  $H$  can act both on the left and on the right to give  $z_R^* \langle z_R | z_R \rangle$  and  $z_R \langle z_R | z_R \rangle$ . When  $z_R$  has nonzero imaginary part,  $\langle z_R | z_R \rangle$  has to be zero [14]. When the norm of a vector is nonzero, no matter how small it is, it can always be normalized. But as long as it has zero norm, it can not be normalized and is not a well-defined state in the Hilbert space. This is what happens here for  $\omega_0 > \omega_{th}$ . When there is no interaction, the discrete state has nonzero norm and can be normalized, and whenever the interaction is turned on its norm vanishes and can not be normalized as usual. The normalization coefficient defined above in Eq. (11) has no probability explanation, since it can be complex. Thus, no compositeness and elementariness with the probability explanation can be defined as usual. In this sense, strictly speaking, Weinberg's original discussion on the compositeness and elementariness for the narrow resonances in [12] is not valid. However, some definitions proposed in the literature such as in [15] might be able to approximately describe the compositeness and elementariness for resonance. In fact, in our opinion, compositeness and elementariness are not physical observables and have no experimental tests, therefore to propose different definitions does not make much physical sense.

#### 4. Dynamically generated states for different partial waves

In above discussions, the continuum states are labeled only by the energy quantum number, which seems to be unrelated to the states in the three dimensional space.

In fact, after partial-wave decomposition of the three dimensional states, the similar nonrelativistic model for the three dimensional states is reduced to a Friedrichs-like model [11]. Since we consider only fixed total angular momentum quantum numbers  $JM$  and fixed  $S$ , by defining  $|0\rangle = |0; JM\rangle$ ,  $|\omega, L\rangle = \sqrt{\mu p} |p; JM; LS\rangle$  and the interaction vertex function  $f(\omega)$ , the total Hamiltonian for one single discrete state coupled with a continuum with a fixed  $JM$  can be cast into

$$H = M_0 |0\rangle\langle 0| + \sum_L \int d\omega \omega |\omega, L\rangle\langle \omega, L| + \sum_L \int d\omega f_L(\omega) |0\rangle\langle \omega, L| + h.c. \quad (14)$$

This is just similar to the original Friedrichs model but with more continua, and the similar exact solution can be obtained.

We can make more generalizations by adding more discrete states and more continuum states, and the interactions between continuum states can also be introduced. The most general Hamiltonian with  $D$  discrete states,  $|i\rangle$  ( $i = 1, \dots, D$ ), and  $C$  continuum states,  $|\omega_j, j\rangle$  ( $j = 1, \dots, C$ ), can be expressed as

$$H = \sum_{i=1}^D M_i |0; i\rangle\langle 0; i| + \sum_{i=1}^C \int_{M_{i,th}}^{\infty} d\omega_i \omega_i |\omega_i; i\rangle\langle \omega_i; i| \quad (15)$$

$$+ \sum_{i_2, i_1} \int_{M_{i_1, th}} d\omega' \int_{M_{i_2, th}} d\omega g_{i_2, i_1}(\omega', \omega) |\omega'; i_2\rangle\langle \omega; i_1| + h.c. \quad (16)$$

$$+ \sum_{i=1}^D \sum_{j=1}^C \int_{M_{j, th}} d\omega f_{i, j}(\omega) |0; i\rangle\langle \omega; j| + h.c. \quad (17)$$

where  $f_{i, j}(\omega)$  is the form factor describing the interaction between the  $i$ th discrete state and the  $j$ th continuum state, and  $g_{ij}$  describes the interaction between the  $i$ th continuum and the  $j$ th continuum. For general interactions  $g_{ij}$ , the model is not solvable, but if  $g_{ij}(\omega', \omega) = v_{ij} f_i(\omega') f_j(\omega)$  and  $f_{ij} = u_{ij} f_j(\omega)$ , where  $u_{ij}$  and  $v_{ij}$  are constant, the model can also be exactly solved. See Ref. [11] for details. Similar separable potential models are also widely used, for example in [16–19]. When there is one more continuum coupled in the system, there will be a new threshold and the Riemann sheets will be doubled. All the poles are also copied to the corresponding new sheets and be renormalized separately, and thus form shadow poles on different sheets with the same origins.

With this formalism we can use a model with only the continuum-continuum interaction but no discrete bare state to look at the behaviors of the dynamically generated states near

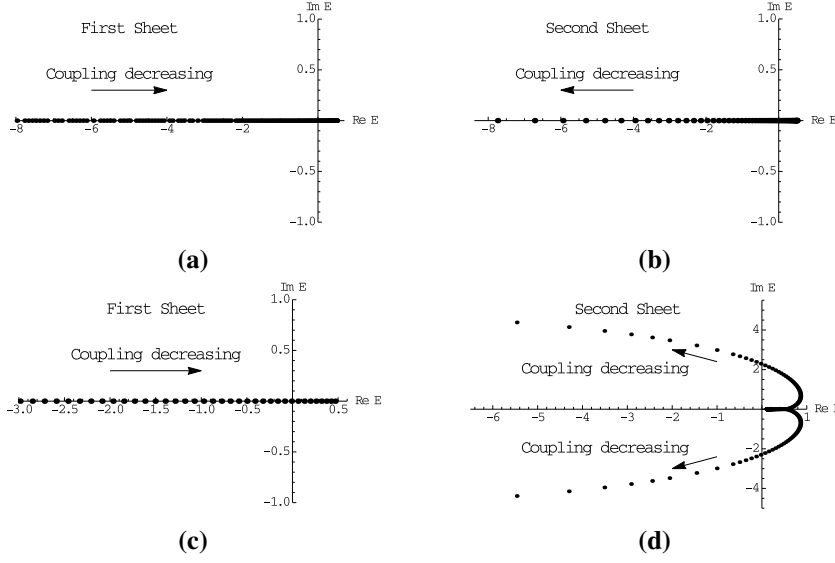


**Figure 3:** (a)(b) illustrate the pole trajectory for the  $S$ -wave states. One bound state move up to the threshold and across the threshold to the second sheet becoming a virtual state as the coupling decreases. (c)(d) illustrate the pole trajectory for the  $P$ -wave state. One bound state and one virtual state merges at the threshold and become a pair of resonance poles

threshold in different partial waves. The Hamiltonian with attractive interaction is

$$H = \int_a d\omega \omega |\omega\rangle\langle\omega| - \lambda^2 \int_a d\omega \int_a d\omega' f(\omega) f^*(\omega') |\omega\rangle\langle\omega'| \quad (18)$$

$$f(\omega) = (\omega - a)^{(l+1/2)/2} \exp\{-(\omega - a)/(2\Lambda)\} \quad (19)$$

Since the behaviors of the form factor near the threshold for different partial waves are universal, we expect that the behaviors of the states near the threshold could be qualitatively correct. The typical  $S$ -wave and  $P$ -wave pole trajectories near the threshold are shown in Fig.3. From this figure we can see that for  $S$ -wave, the bound state near the threshold could appear by itself, and as the coupling decreases, it moves up across the threshold to the second sheet and become a virtual state. In the  $P$ -wave, we see that the bound state and the virtual state appear together and as the coupling decreases, they meet at the threshold to become a pair of resonance poles. This behavior near the threshold is also typical for the higher partial waves. This difference for  $S$ -wave and higher partial waves were also discussed in [20] using the effective range expansion and also in [21] using the Jost function. Recall that with the weak coupling, when  $\omega_0 < \omega_{th}$ , the bare state generates a bound state and a virtual state, which is similar to the cases for the higher partial waves. But the bound state in the  $S$ -wave seems different, it could have no accompanied near threshold virtual state. This is a demonstration of the so called pole-counting rule proposed by Morgan [22, 23] and used in the determination of the exotic states [24]. However, the virtual-bound pair generated from the bare state locates close to each other only at weak couplings. When the coupling is strong, this rule may not be a solid criterion.

## 5. Relativistic generalization: Friedrichs-Lee model

In the non-relativistic Friedrichs model, we see that the integral in  $\eta(\omega)$  is in terms of energy. But we know that for relativistic theory, the corresponding dispersion relations are expressed in terms of the Lorentz invariant  $s \sim E^2$ . This is because in the non-relativistic theory, the negative frequency part or the antiparticles are not taken into account. There are several ways to incorporate the relativistic effects into the Friedrichs model in a systematical way [25, 26] and we will follow the method in [26] which is direct and simple by introducing a bilocal operator to simulate the two-particle state. The creation operator for the bare discrete state is  $a_{\mathbf{p}jm}^\dagger$  with  $[a_{\mathbf{p}jm}, a_{\mathbf{p}'j'm'}^\dagger] = \delta^{(3)}(\mathbf{p} - \mathbf{p}')\delta_{jj'}\delta_{mm'}$ . The bilocal field approach makes a little more simplification than Lee-model by describing the two-particle continuum using one set of creation and annihilation operator  $B(E, \mathbf{p}), B^\dagger(E, \mathbf{p})$  with the commutator  $[B(E, \mathbf{p}), B^\dagger(E', \mathbf{p}')] = \delta^{(3)}(\mathbf{p} - \mathbf{p}')\beta(E)^{-1}\delta(E - E')$ . Then, the Hamiltonian can be expressed as

$$P_0 = \int d^3\mathbf{p}\omega(\mathbf{p})a^\dagger(\mathbf{p})a(\mathbf{p}) + \int d^3\mathbf{p}k^2dkE(\mathbf{p}, \mathbf{k})B^\dagger(\mathbf{p}, k)B(\mathbf{p}, k) \\ + \int d^3\mathbf{p}k^2dk\alpha(k)(a(\mathbf{p}) + a^\dagger(-\mathbf{p}))(B^\dagger(\mathbf{p}, k) + B(-\mathbf{p}, k)), \quad (20)$$

where we omitted the angular momentum quantum number for simplicity. The energy of the free single-particle state is  $\omega(\mathbf{p}) = (\mathbf{p}^2 + \omega_0^2)^{1/2}$  and the total energy of the free two-particle state is  $E(\mathbf{p}, \mathbf{k}) = (\mathbf{p}^2 + W(\mathbf{k})^2)^{1/2}$  with the c.m. energy defined by  $W(\mathbf{k}) = \varepsilon_1(\mathbf{k}) + \varepsilon_2(-\mathbf{k})$ . The coupling vertex,  $\alpha(k)$ , represents the interaction between the single-particle state and the two-particle state [27]. Then to solve the eigenvalue problem is to find the new ladder operators  $b^\dagger(E, \mathbf{p})$  solution for the equation

$$[P_\mu, b^\dagger(E, \mathbf{p})] = p_\mu b^\dagger(E, \mathbf{p}), \quad (21)$$

in terms of  $B^\dagger(E, \mathbf{p}), B(E, -\mathbf{p}), a^\dagger(\mathbf{p})$ , and  $a(-\mathbf{p})$ . This can be exactly solved as the nonrelativistic one. The  $\eta$  function can now be expressed using the relativistic invariant  $s$

$$\eta_\pm(s) = s - \omega_0^2 - \int_{s_{th}} ds' \frac{\rho(s')}{s - s' \pm i0}, \quad (22)$$

where in center of mass system  $\rho(W) = 2\omega_0\beta(W)\alpha(k)^2 = 2\omega_0\frac{k\varepsilon_1\varepsilon_2}{W}\alpha(k)^2$ ,  $\rho(s) \equiv 2\omega(\mathbf{p})\beta(E')\alpha(k(E', \mathbf{p}))^2$ . The pole position for the discrete state can be obtained by solving  $\eta(s) = 0$ , where  $\eta(s)$  is the analytically continued  $\eta_\pm$  on the complex  $s$ -plane. Similarly, the bound state, virtual state, resonance solutions can be obtained at the zero points of  $\eta(s)$ . For completeness, we list only the creation operators for the bound states

$$b^\dagger(E_0, \mathbf{p}) = N \left[ \frac{(\omega(\mathbf{p}) + E_0)}{\sqrt{2\omega(\mathbf{p})}} a^\dagger(\mathbf{p}) - \frac{(\omega(\mathbf{p}) - E_0)}{\sqrt{2\omega(\mathbf{p})}} a(-\mathbf{p}) \right. \\ \left. - \sqrt{2\omega(\mathbf{p})} \int_{M_{th}} dE' \beta(E') \left[ \frac{\alpha(k(E', \mathbf{p}))}{E' - E_0} B^\dagger(E', \mathbf{p}) - \frac{\alpha(k(E', \mathbf{p}))}{E' + E_0} B(E', -\mathbf{p}) \right] \right]. \quad (23)$$

All the forgoing discussions in the nonrelativistic model apply also in the relativistic model.

## 6. Application: Nonrelativistic Friedrichs-QPC scheme

The Friedrichs model can not only clarify some conceptual problem, but also can have applications in real hadronic physics where there is interaction between discrete states and continuum states. We will restrict our study on the properties of mesons.

To apply this model, one has to determine the interaction between the discrete meson state and the two-meson continuum state from the real dynamics instead of putting it by hand. We first consider the non-relativistic cases. Here, we use the QPC model [28] to model this kind of interaction. In this model, the meson coupling  $A \rightarrow BC$  can be defined as the transition matrix element

$$\langle BC|T|A\rangle = \delta^3(\vec{P}_f - \vec{P}_i)\mathcal{M}^{ABC} \quad (24)$$

where the transition operator  $T$  in the QPC model describes the quark-antiquark pair generation from the vacuum and  $|A\rangle, |B\rangle, |C\rangle$  are the Mock states for the mesons [28]. By the standard derivation one can obtain the amplitude  $\mathcal{M}^{ABC}$  defined by Eq. (24) and the partial-wave amplitude  $\mathcal{M}^{SL}(P(\omega))$  as in Ref. [28]. Then the vertex  $f_{SL}$  which describes the interaction between  $|A\rangle$  and  $|BC\rangle$  in the Friedrichs model can be obtained. The bare masses and radial wave functions of the meson states in the QPC model can be given by the GI model [2]. Then this Friedrichs-QPC scheme can be viewed as including the hadron loop correction to the Godfrey-Isgur's results.

Now we have set up the basic scheme and it can be used to study some physical hadronic spectra where there are interactions between discrete states and continuum states. In ref. [29], we discussed the charmonium like spectra in the  $2^3P_{0,1,2}$  and  $2^1P_1$  sectors. By coupling the quarkonium states in these four channels with the corresponding continua states using the QPC model with the wave function from GI, we can calculate the interaction vertex. Only the OZI allowed channels are included up to  $D^*\bar{D}^*$ . Then by solving the  $\eta(\omega) = 0$  from the Friedrichs model we can find out the discrete states in these four channels. The results are listed in table (1). It is important to emphasize that the interaction vertex is totally given by the dynamics from the QPC model with only one free parameter  $\gamma$ .

From the result, we see that the famous  $X(3872)$  appears as the dynamically generated bound state by the interaction between the  $2^3P_1$  charmonium and the  $D\bar{D}^*, D^*\bar{D}^*$  continua. The  $D\bar{D}^*$  component is found to be the dominant one. The original  $\chi_{c1}$  moves to the second sheet and become a resonance which may be related to the  $X(3940)$ . Similar results were also found in [31, 32]. The  $\chi_{c0}$  state is strange. Its interaction to the  $D\bar{D}$  is smaller than the one to the  $D^*\bar{D}^*$ . It is this strong  $D^*\bar{D}^*$  coupling which drags the  $\chi_{c0}$  state down to around 3860 MeV.

**Table 1:** Comparison of the experimental masses and the total widths (in MeV) [30] with our results.

$n^{2s+1}L_J$	$M_{expt}$	$\Gamma_{expt}$	$M_{BW}$	$\Gamma_{BW}$	pole	GI
$2^3P_2$	$3927.2 \pm 2.6$	$24 \pm 6$	3920	10	3920-4i	3979
$2^3P_1$	$3942 \pm 9$	$37^{+27}_{-17}$			3934-40i	3953
	$3871.69 \pm 0.17$	$< 1.2$	3871	0	3871-0i	
$2^3P_0$	$3862^{+66}_{-45}$	$201^{+242}_{-149}$	3878	11	3878-5i	3917
$2^1P_1$			3895	37	3902-27i	3956

## 7. Application: two-pole structures in hadron spectra

In previous discussions, we notice that by coupling the discrete state with the continuum, there could be new state dynamically generated and together with the original one they could form the two-pole structure. The dynamically generated pole is also called the ‘‘companion pole’’ [33]. Such a phenomenon has been seen in the literature in different situations [19, 31, 32, 34–41]. This phenomenon may be a general one and appears not only in the heavy quark system but also in the low lying states with light quarks.

The lightest  $0^+$  scalars  $f_0(500)$ ,  $K_0^*(700)$ ,  $a_0(980)$ , and  $f_0(980)$  are suggested to be non- $q\bar{q}$  states. More recently, some hadron states with heavy quarks, such as  $D_0^*(2300)$ ,  $D_{s0}^*(2317)$ , are also puzzling states which could hardly be accommodated in the predicted  $q\bar{q}$  states in the quark potential model. With relativistic Friedrichs model we can study whether these states can be dynamically generated by the above mechanism. These dynamically generated states may combine with the bare seed states and form two-pole structures. To describe both the light scalars and the ones with heavy quarks, the relativistic QPC model by Fuda [42] is used here. Some predictions on the corresponding states with  $b$  quarks can also be made. Our results from Ref. [42, 43] is shown in Tab.2. Similar two-pole structures are also found in the Unitarized  $H\chi$ PT approach [44–46], however, with different origins.

## 8. Conclusion

The Friedrichs model as a solvable model can give an explicit expression of the bound states, virtual states, and resonances, and helps us in understanding different states in the hadron physics. From this discussion, we understood why the virtual states and resonances can not be normalized and can not have a good definition of the compositeness and elementariness. In order to understand the origin of the dynamically generated states, we also show some examples where some states can be dynamically generated from the singularities of the form factors. Different behaviors for the near-threshold dynamically generated states in different partial waves are also discussed. Combined with QPC model,

**Table 2:** Correspondence of the discrete states and the continuum states as the parameter  $\gamma = 4.3\text{GeV}$ . The values in the fourth column are the input mass of bare states. Unit is GeV.

"discrete"	"continuum"	GI mass	Input	poles	experiment states	PDG values [47]
$\frac{u\bar{u}+d\bar{d}}{\sqrt{2}}(1^3P_0)$	$(\pi\pi)_{I=0}$	1.09	1.3	$\sqrt{s_{r1}} = 1.34 - 0.29i$ $\sqrt{s_{r2}} = 0.39 - 0.26i$	$f_0(1370)$ $f_0(500)$	$1.35^{±0.15} - 0.2^{±0.05}i$ $0.475^{±0.075} - 0.275^{±0.075}i$
$u\bar{s}(1^3P_0)$	$(\pi K)_{I=\frac{1}{2}}$	1.23	1.42	$\sqrt{s_{r1}} = 1.41 - 0.17i$ $\sqrt{s_{r2}} = 0.66 - 0.34i$	$K_0^*(1430)$ $K_0^*(700)$	$1.425^{±0.05} - 0.135^{±0.04}i$ $0.68^{±0.05} - 0.30^{±0.04}i$
$s\bar{s}(1^3P_0)$	$K\bar{K}$	1.35	1.68	$\sqrt{s_{r1}} = 1.71 - 0.16i$ $\sqrt{s_B} = 0.98, \sqrt{s_V} = 0.19$	$f_0(1710)$ $f_0(980)$	$1.704^{±0.012} - 0.062^{±0.009}i$ $0.99^{±0.02} - 0.028^{±0.023}i$
$\frac{u\bar{u}-d\bar{d}}{\sqrt{2}}(1^3P_0)$	$\pi\eta$	1.09	1.3	$\sqrt{s_{r1}} = 1.26 - 0.14i$ $\sqrt{s_{r2}} = 0.70 - 0.42i$	$a_0(1450)$ $a_0(980)$	$1.474^{±0.019} - 0.133^{±0.007}i$ $0.98^{±0.02} - 0.038^{±0.012}i$
$c\bar{u}(1^3P_0)$	$D\pi$	2.4	2.4	$\sqrt{s_{r1}} = 2.58 - 0.24i$ $\sqrt{s_{r2}} = 2.08 - 0.10i$	$D_0^*(2300)$	$2.30^{±0.019} - 0.137^{±0.02}i$
$c\bar{s}(1^3P_0)$	$DK$	2.48	2.48	$\sqrt{s_{r1}} = 2.80 - 0.23i$ $\sqrt{s_B} = 2.24, \sqrt{s_V} = 1.8$	$D_{s0}^*(2317)$	$2.317^{±0.0005} - 0.0038^{±0.0038}i$
$b\bar{u}(1^3P_0)$	$\bar{B}\pi$	5.76	5.76	$\sqrt{s_{r1}} = 6.01 - 0.21i$ $\sqrt{s_{r2}} = 5.56 - 0.07i$		
$b\bar{s}(1^3P_0)$	$\bar{B}K$	5.83	5.83	$\sqrt{s_{r1}} = 6.23 - 0.17i$ $\sqrt{s_B} = 5.66, \sqrt{s_V} = 5.3$		
$c\bar{c}(2^3P_1)$	$D\bar{D}^*$	3.95	3.95	$\sqrt{s_{r1}} = 4.01 - 0.049i$ $\sqrt{s_B} = 3.785$	$X(3940)$ $X(3872)$	$3.87169^{±0.00017}$

this model can be used in the discussion of the properties of the hadronic states. In particular, we have shown that  $X(3872)$  could be the dynamically generated state by the interaction of the bare  $2^3P_1 c\bar{c}$  state and the continua. The  $X(3872)$  and the state generated from the bare  $c\bar{c}$  state form a two-pole structure. This two-pole structure may be a general phenomenon in hadron physics. We also show some other examples to demonstrate this kind of two-pole structure.

## Acknowledgments

This work is supported by National Science Foundation of China under contract Nos. 11975075 and 11575177. ZX is also supported by “the Fundamental Research Funds for the Central Universities”.

## References

- [1] E. Eichten, K. Gottfried, T. Kinoshita, K. D. Lane, and Tung-Mow Yan. Charmonium: The Model. *Phys. Rev.*, D 17:3090, 1978. [Erratum: *Phys. Rev.*D 21,313(1980)].
- [2] S. Godfrey and Nathan Isgur. Mesons in a Relativized Quark Model with Chromodynamics. *Phys. Rev.*, D 32:189–231, 1985.
- [3] K. O. Friedrichs. On the perturbation of continuous spectra. *Commun. Pure Appl. Math.*, 1(4):361–406, 1948.
- [4] P. Facchi, H. Nakazato, and S. Pascazio. From the quantum zeno to the inverse quantum zeno effect. *Phys. Rev. Lett.*, 86:2699–2703, Mar 2001.

- [5] E. T. Jaynes and F. W. Cummings. Comparison of quantum and semiclassical radiation theories with application to the beam maser. *Proc. IEEE*, 51:89, 1963.
- [6] T. D. Lee. Some Special Examples in Renormalizable Field Theory. *Phys. Rev.*, 95:1329–1334, 1954.
- [7] Francesco Giacosa. Non-exponential decay in quantum field theory and in quantum mechanics: the case of two (or more) decay channels. *Found. Phys.*, 42:1262–1299, 2012.
- [8] Pok Man Lo and Francesco Giacosa. Thermal contribution of unstable states. *Eur. Phys. J. C*, 79(4):336, 2019.
- [9] Zhiguang Xiao and Zhi-Yong Zhou. Virtual states and the generalized completeness relation in the Friedrichs model. *Phys. Rev., D* 94(7):076006, 2016.
- [10] Zhiguang Xiao and Zhi-Yong Zhou. On Friedrichs Model with Two Continuum States. *J. Math. Phys.*, 58(6):062110, 2017.
- [11] Zhiguang Xiao and Zhi-Yong Zhou. Partial Wave Decomposition in Friedrichs Model With Self-interacting Continua. *J. Math. Phys.*, 58(7):072102, 2017.
- [12] Steven Weinberg. Elementary particle theory of composite particles. *Phys. Rev.*, 130:776–783, 1963.
- [13] T. Petrosky, I. Prigogine, and S. Tasaki. Quantum theory of non-integrable systems. *Physica*, 173A(1-2):175–242, 1991.
- [14] Noboru Nakanishi. A theory of clothed unstable particles. *Prog. of Theor. Phys.*, 19(6):607–621, 1958.
- [15] Zhi-Hui Guo and J. A. Oller. Probabilistic interpretation of compositeness relation for resonances. *Phys. Rev., D* 93(9):096001, 2016.
- [16] Steven Weinberg. Quasiparticles and the Born Series. *Phys. Rev.*, 131:440–460, 1963.
- [17] E. Hernández and A. Mondragón. Resonant states in momentum representation. *Phys. Rev., C* 29:722–738, 1984.
- [18] F. Aceti and E. Oset. Wave functions of composite hadron states and relationship to couplings of scattering amplitudes for general partial waves. *Phys. Rev., D* 86:014012, 2012.
- [19] Takayasu Sekihara, Tetsuo Hyodo, and Daisuke Jido. Comprehensive analysis of the wave function of a hadronic resonance and its compositeness. *PTEP*, 2015:063D04, 2015.

- [20] C. Hanhart, J. R. Pelaez, and G. Rios. Remarks on pole trajectories for resonances. *Phys. Lett.*, B739:375–382, 2014.
- [21] Tetsuo Hyodo. Hadron mass scaling near the  $s$ -wave threshold. *Phys. Rev. C*, 90:055208, Nov 2014.
- [22] D. Morgan. Pole counting and resonance classification. *Nucl. Phys.*, A543:632–644, 1992.
- [23] V. Baru, J. Haidenbauer, C. Hanhart, Yu. Kalashnikova, and Alexander Evgenyevich Kudryavtsev. Evidence that the  $a(0)(980)$  and  $f(0)(980)$  are not elementary particles. *Phys. Lett. B*, 586:53–61, 2004.
- [24] Ou Zhang, C. Meng, and H. Q. Zheng. Ambiversion of  $X(3872)$ . *Phys. Lett.*, B680:453–458, 2009.
- [25] L.P. Horwitz. The Unstable system in relativistic quantum mechanics. *Found. Phys.*, 25:39–65, 1995.
- [26] I. Antoniou, M. Gadella, I. Prigogine, and G. P. Pronko. Relativistic Gamow vectors. *J. Math. Phys.*, 39:2995, 1998.
- [27] Zhi-Yong Zhou and Zhiguang Xiao. Relativistic Friedrichs-Lee model and quark-pair creation model. *Eur. Phys. J. C*, 80:1191, 2020.
- [28] Harry G. Blundell and Stephen Godfrey. The  $\xi$  (2220) revisited: Strong decays of the  $1^3F_2$   $1^3F_4$   $s$  anti- $s$  mesons. *Phys. Rev.*, D 53:3700–3711, 1996.
- [29] Zhi-Yong Zhou and Zhiguang Xiao. Understanding  $X(3862)$ ,  $X(3872)$ , and  $X(3930)$  in a Friedrichs-model-like scheme. *Phys. Rev.*, D96(5):054031, 2017. [Erratum: *Phys. Rev. D* 96, 099905 (2017)].
- [30] C. Patrignani et al. Review of Particle Physics. *Chin. Phys.*, C40(10):100001, 2016.
- [31] Susana Coito, George Rupp, and Eef van Beveren.  $X(3872)$  is not a true molecule. *Eur. Phys. J.*, C73(3):2351, 2013.
- [32] Francesco Giacosa, Milena Piotrowska, and Susana Coito.  $X(3872)$  as virtual companion pole of the charm-anticharm state  $\chi_{c1}(2P)$ . 2019.
- [33] M. Boggione and M.R. Pennington. Dynamical generation of scalar mesons. *Phys. Rev. D*, 65:114010, 2002.
- [34] E. van Beveren, T.A. Rijken, K. Metzger, C. Dullemond, G. Rupp, and J.E. Ribeiro. A Low Lying Scalar Meson Nonet in a Unitarized Meson Model. *Z. Phys. C*, 30:615–620, 1986.

- [35] Eef van Beveren and George Rupp. Modern meson spectroscopy: the fundamental role of unitarity. *Prog. Part. Nucl. Phys.*, 117:103845, 2021.
- [36] Nils A. Tornqvist. Understanding the scalar meson  $q$  anti- $q$  nonet. *Z. Phys.*, C68:647–660, 1995.
- [37] Yu. S. Kalashnikova. Coupled-channel model for charmonium levels and an option for  $X(3872)$ . *Phys. Rev.*, D72:034010, 2005.
- [38] P. G. Ortega, J. Segovia, D. R. Entem, and F. Fernandez. Coupled channel approach to the structure of the  $X(3872)$ . *Phys. Rev.*, D81:054023, 2010.
- [39] Makoto Takizawa and Sachiko Takeuchi.  $X(3872)$  as a hybrid state of charmonium and the hadronic molecule. *PTEP*, 2013:093D01, 2013.
- [40] Zhi-Yong Zhou and Zhiguang Xiao. Comprehending Isospin breaking effects of  $X(3872)$  in a Friedrichs-model-like scheme. *Phys. Rev.*, D97(3):034011, 2018.
- [41] Susana Coito and Francesco Giacosa. Line-shape and poles of the  $\psi(3770)$ . *Nucl. Phys. A*, 981:38–61, 2019.
- [42] Michael G. Fuda. Relativistic quantum mechanics and the quark-pair creation model. *Phys. Rev. C*, 86:055205, 2012.
- [43] Zhi-Yong Zhou and Zhiguang Xiao. Two-pole structures in a relativistic Friedrichs–Lee-QPC scheme. *Eur. Phys. J. C*, 81(6):551, 2021.
- [44] Zhi-Hui Guo, Ulf-G. Meißner, and De-Liang Yao. New insights into the  $D_{s0}^*(2317)$  and other charm scalar mesons. *Phys. Rev. D*, 92(9):094008, 2015.
- [45] Miguel Albaladejo, Pedro Fernandez-Soler, Feng-Kun Guo, and Juan Nieves. Two-pole structure of the  $D_0^*(2400)$ . *Phys. Lett. B*, 767:465–469, 2017.
- [46] Ulf-G. Meißner. Two-pole structures in QCD: Facts, not fantasy! *Symmetry*, 12(6):981, 2020.
- [47] M. Tanabashi et al. Review of Particle Physics. *Phys. Rev. D*, 98(3):030001, 2018.